THE JOURNAL OF PHYSICAL CHEMISTRY B

Article

pubs.acs.org/JPCB

Effect of Rod Length on the Morphology of Block Copolymer/Magnetic Nanorod Composites

Chieh-Tsung Lo* and Wei-Ting Lin

Department of Chemical Engineering, National Cheng Kung University, No. 1, University Road, Tainan City 701, Taiwan

ABSTRACT: The organization of magnetic nanorods in microphase-separated diblock copolymers composed of poly(styrene-*b*-2-vinylpyridine) (PS-PVP) as a function of rod length and rod concentration was investigated using both transmission electron microscopy and small-angle X-ray scattering. Our results reveal that the nanorods were sequestered into the PVP domains, which is attributed to the preferential interaction between pyridine-tethered nanorods and PVP. Meanwhile, the addition of nanorods in PS-PVP caused chain stretching. To minimize the energy penalty, nanorods tended to align parallel to the interface between PS and PVP to increase the conformational entropy. As the length of nanorods increased, the increasing van der Waals interaction and magnetic interaction caused extensive rod aggregation, which suppressed the domain size of PVP and amplified the local compositional fluctuations. This creates conditions to induce disorder in the polymer morphology and nanorods undergo macrophase separation.

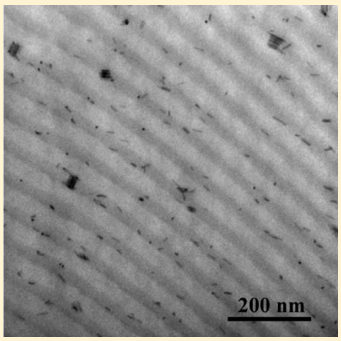

INTRODUCTION

Magnetic nanoparticles are of great interest in the scientific community because of their potential applications in nanotechnology, including data storage media,[1,2] spin-dependent electron transport devices,[3] therapeutic or diagnostic medical functions,[4,5] and environmental remediation.[6,7] When magnetic particles are in the length scale of nanometer, each particle exhibits a constant magnetic moment and shows a fast response to an applied magnetic field. In addition, the particle size, interparticle separation, functionalized surface, and surface oxidation have huge influence on the magnetic properties of particles.[8] Significant efforts have been devoted to synthesizing well-dispersed magnetic nanoparticles. Among these studies, a novel technique using block copolymer as a template to organize magnetic nanoparticles in an ordered array is developed.[9−14] This method lies in the rich diversity of nanostructures of block copolymers that provide an effective means for controlling magnetic particle dispersion. The spatially organized magnetic nanoparticles have the potential to address the huge demand for the wide range of applications.

Many works have reported the synthesis and phase behavior of nonmagnetic spherical nanoparticles in block copolymer.[15−22] Most of the strategies utilized the chemically modified nanoparticles to be selective to the one domain of block copolymer. While block copolymers exhibit microphase separation and form a wide range of morphologies such as lamellae, gyroid, hexagonally packed cylinders, and spheres,[23] the tailored nanoparticles can then be organized into unique 2D or 3D spatial distribution. The morphology of these block copolymer/nanoparticle composites can be tuned by both the volume fraction of two microdomains[24,25] and the physical properties of nanoparticles including particle size,[15,26−28] concentration,[22,27] and the grafting materials on nanoparticles.[29,30] Furthermore, the relative location of particles either in the preferred domain or at the interface of block copolymer can be controlled by varying the particle size and the length of the tethered polymer on the particles.[15,27,28] However, when the particle size is comparable to the root-mean-square end-to-end distance of the preferred block, particles segregate to a particle-rich core, surrounded by an ordered polymer structure.[31] These studies have demonstrated the effectiveness of leveraging the rich phase behavior of the block copolymer for ordering the nonmagnetic nanoparticles in polymer matrices. In comparison with the block copolymer/nonmagnetic nanoparticle composites, the synthesis of block copolymer/magnetic particle composites is even more challenging because the magnetic interaction between particles makes it difficult to prepare composites without particle aggregation. Composto et al. investigated the dispersion of polymer-grafted Fe_3O_4 nanoparticles in block copolymer.[13,14] At a fixed grafting density of surfactants on the surface of particles, a uniform dispersion of particles was obtained at low brush lengths. Upon increasing brush molecular weight, nanoparticles were driven into large aggregates. As a result, the block copolymer assembled into onionlike rings around particle aggregates. Park et al. found that the strong particle−particle interaction between γ-Fe_2O_3 nanoparticles caused lattice-like aggregates.[12] These aggregates further induced a morphological transition of block copolymer from hexagonally packed cylinders to body-center-cubic spheres via undulated cylinders. This transition is different from the traditionally morphological transition of neat block copolymer. To maximize the selectivity of magnetic nanoparticles in the preferred domains of block copolymer and to achieve isolated single particles in a media, Darling et al. employed a vacuum ultraviolet radiation approach to create coverage in a block copolymer template.[10] Further deposition

Received: September 3, 2012
Revised: April 12, 2013
Published: April 12, 2013

dx.doi.org/10.1021/jp308723q | *J. Phys. Chem. B* 2013, 117, 5261−5270

of nanoparticles led to the spatial ordering of magnetic particles within the channels.

The magnetization of magnetic nanoparticles shows a strong function of the particle shape. The great enhancement in the coercivity is found from 820 to 10 100 Oe with an increase in the aspect ratio of Fe particles from 1.1 to 10.[32] Thus, the synthesis and phase behavior of block copolymer/magnetic nanorod mixtures are even more intriguing. In order to accommodate nonspherical nanoparticles in an ordered structure, at least one of the microdomain dimensions should be equal to or larger than one of the particle dimensions to prevent large energy penalty caused by the associated chain conformational distortions.[33] To gain a better insight into the thermodynamic aspects of organizing nanorods in ordered microphase-separated domains of block copolymer, several theoretical studies have been carried out. Chen and Ma used a coarse-grained description of a microphase-separating A-B block copolymer to simulate the growth kinetics of phase separation of block copolymer/noninteracting nanorod composites.[34] They found that the phase ordering process was associated with the movement of rods. Additionally, the self-assembly of rods on the copolymer scaffold produced highly ordered nanowires. Using a dissipative particle dynamics method, He et al. investigated the self-assembly of block copolymer blended with mono- or bidispersed noninteracting nanorods.[35] The results showed that the equilibrium morphology of composites depends strongly on the rod concentration, rod length, and the interaction strength between blocks and rods. When bidispersed nanorods were mixed with block copolymer, longer nanorods preferentially located at the interface between two microdomains, whereas shorter nanorods occupied the center of the preferred domains with a lower concentration at the interface. On the experimental front, Deshmukh et al. investigated the confinement of noninteracting nanorods in block copolymer domains and showed that the orientation of nanorods in the preferred domains could be controlled by choosing an appropriate polymer domain size relative to nanorod dimensions.[36] The orientation of noninteracting nanorods could also be controlled by a stretch film method in which nanorods rotated and aligned along the stretch direction in response to the trench created by polymer deformation.[37]

In the present study, we investigated the effect of interacting nanorods on the phase behavior of block copolymer/nanorod composites. While even obtaining a good dispersion of noninteracting nanorods in polymer matrices has been a challenge, it is far more formidable to tailor the magnetic nanorods in block copolymer. In addition, since the magnetic properties of these composites strongly depend on the nature of dispersion and ordering of rods in the polymer matrices, tailoring nanorods into arrays in ordered polymer phase will provide exciting new possibilities on the materials front. To the best of our knowledge, this is the first effort to synthesize the block copolymer/magnetic nanorod composites and address the phase behavior upon the incorporation of nanorods into block copolymer. To gain a better insight into the thermodynamic aspects of dispersing nanorods in a polymer matrix, we first establish the miscibility of nanorods within the PVP domains in block copolymer via studying the dispersion of nanorods in PVP homopolymer with the molecular weight comparable to the PVP domain. This information is crucial to further investigate the rod dispersion in block copolymer. Our study on block copolymer/nanorod composites clearly shows the effect of rod length in causing dramatic shifts on both the order−disorder transition of the block copolymer/nanorod composite and rod dispersion. This effect is caused by the interplay between the van der Waals interaction, magnetic interaction, and the conformational entropy of block copolymer. Given that the literature is scarce with both the experimental and simulation data on the assembly of the interacting nanorods in block polymer, we believe that this study can provide guidance to such experiments by identifying the key physical variables to achieve good rod dispersion and control morphology of composite materials.

EXPERIMENTAL SECTION

Fe_2P nanorods were prepared according to published procedures.[38] Briefly, 0.3 g of $Fe(CO)_5$ (>97%, Sigma-Aldrich Co.) and 4.8 g of trioctylphosphine (TOP, Sigma-Aldrich Co.) were mixed at 100 °C. The stock solution was quickly injected into 5.0 g of preheated trioctylphosphine oxide (TOPO, Sigma-Aldrich Co.) at 340 °C under argon atmosphere, and aged for various reaction times. As-prepared nanorods were purified by the addition of excess acetone to remove the residual ions and unreacted chemicals.

Pyridine-tethered Fe_2P nanorods were prepared through a ligand exchange process according to Gupta et al.[39] The alkane-covered rods were refluxed in 10 mL of anhydrous pyridine (Sigma-Aldrich Co.) at 100 °C for 24 h and then purified by precipitation in hexane. These pyridine-tethered nanorods were redispersed in 10 mL of THF (~100%, J. T. Baker) for the preparation of composites. Weight fractions of rods and ligands were measured by thermal gravimetric analysis (TGA). The weight fraction of residue during thermal analysis was assumed to be that of the pure rods. The number of ligands per each rod divided by the average surface area of the rods gives the chain areal density of ligands on particle surface.[40,41]

As-prepared nanorods were mixed with poly(2-vinylpyridine) (PVP, Polymer Source, Inc.) with the number-averaged molecular weight (M_n) of 97 000 g/mol and PDI = 1.08 in THF to prepare PVP/nanorod composite. This mixture was stored at ambient condition for at least 2 days. The complex solution was then cast on epoxy resin to prepare bulk composite. After drying in vacuum, the specimen was annealed at 180 °C for 7 days. An Ultracut R microtome (Reichert, Leica, MI) was used to section the embedded samples in epoxy to a thickness of ~80 nm. The distribution of nanorods in PVP was analyzed using a Hitachi H7500 transmission electron microscope operated at 100 kV.

To prepare block copolymer/nanorod composites, the pyridine-tethered nanorods were mixed with poly(styrene-*b*-2-vinylpyridine) (PS-PVP, M_n of PS and PVP = 102 000 and 97 000 g/mol respectively, PDI = 1.12, Polymer Source, Inc.) in THF. The composites were both embedded in epoxy and cast on Kapton. Samples were then annealed at 180 °C for 7 days, and microtomed to ~80 nm thickness. The PVP domains were stained selectively using an iodine vapor. The organization of nanorods in PS-PVP was analyzed using the same transmission electron microscope. The images were acquired over different areas of the same and duplicate specimens. The distribution and location of rods were determined by analyzing many TEM images.

To complement the TEM results, small-angle X-ray scattering (SAXS) measurements were performed at both Sector 23A1 at the National Synchrotron Radiation Research Center in Taiwan and a Bruker diffractometer (NanoSTAR U

dx.doi.org/10.1021/jp308723q | J. Phys. Chem. B 2013, 117, 5261−5270

System, Bruker AXS Gmbh, Karlsruhe, Germany). Samples on Kapton were measured at room temperature with a sample to detector distance of 2 m. The data were corrected for incident flux, absorption, detector sensitivity variation, and dark current.

RESULTS AND DISCUSSION

Characterization of Nanorods. Figure 1 shows the nanorods synthesized via thermal decomposition for different

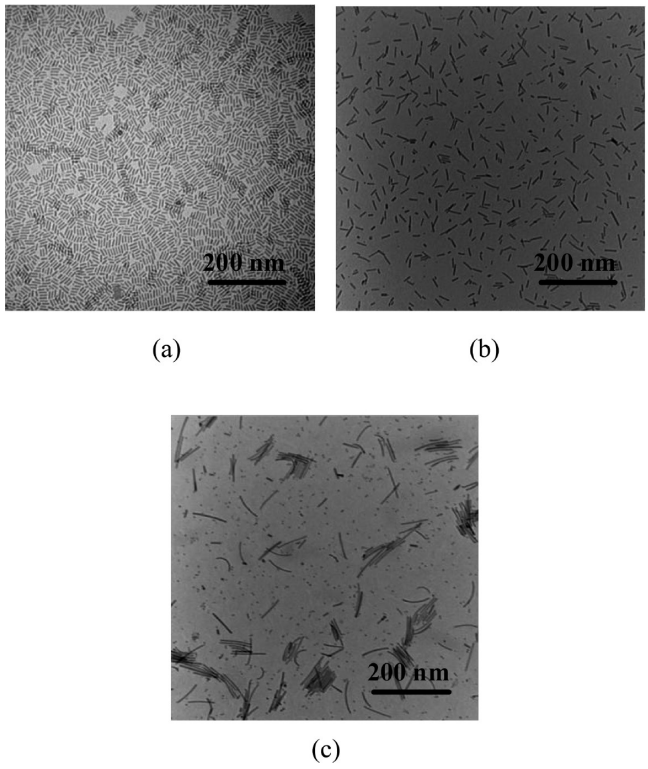

Figure 1. TEM images of nanorods prepared for different reaction times: (a) 30 min; (b) 60 min; and (c) 90 min.

reaction times. The length of nanorods increased from ~20.9 ± 2.9 nm to ~40.8 ± 5.7 nm and 100.9 ± 7.5 nm for 30 min, 60 min, and 90 min, respectively, whereas the diameter of nanorods (~ 4.5 nm) was almost identical for different reaction times. With surface modification using pyridine, the areal density of pyridine chains on the rod surface is 3.70 chains/nm^2, 3.85 chains/nm^2, and 2.90 chains/nm^2 for nanorods with rod length of 20.9 nm, 40.8 nm, and 100.9 nm, respectively.

Dispersion of Nanorods in Homopolymer. We first establish the miscibility of nanorods within the PVP domains in block copolymer via studying the dispersion of nanorods in PVP homopolymer with the molecular weight comparable to the PVP domain. Figure 2 shows the cross-sectional TEM images of 20.9 nm long nanorods in PVP. The nanorods were well distributed in the PVP matrix and no aggregation was observed at the weight fraction of nanorods (ϕ) up to 4%. When nanorods with a rod length of 40.8 nm were incorporated into PVP (Figure 3), the dispersion of nanorods was similar to that with the smaller rod length. There was no significant rod aggregation at both low and high particle loading.

Figure 4 shows representative TEM images of nanorods with a length of 100.9 nm incorporated into PVP. Unlike the

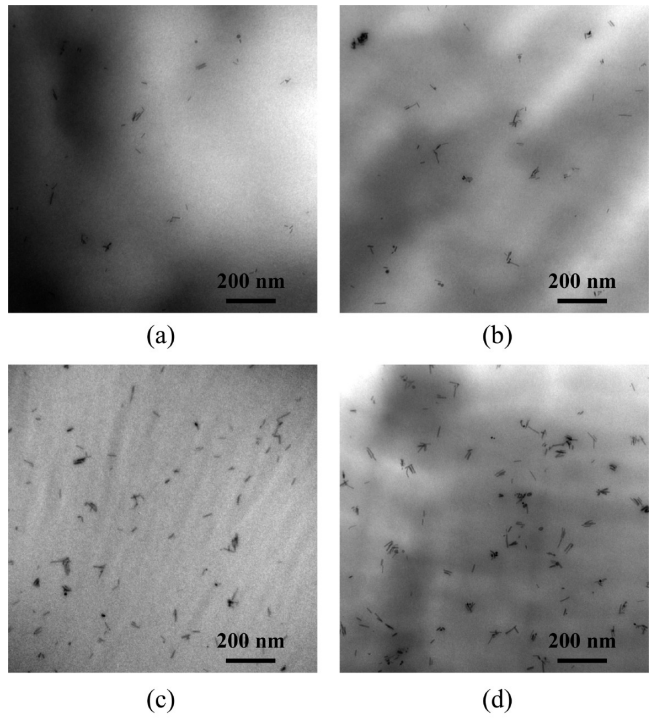

Figure 2. Dispersion of nanorods in PVP: (a) ϕ = 0.5%; (b) ϕ = 1%; (c) ϕ = 2%; and (d) ϕ = 4%. The rod length is 20.9 nm.

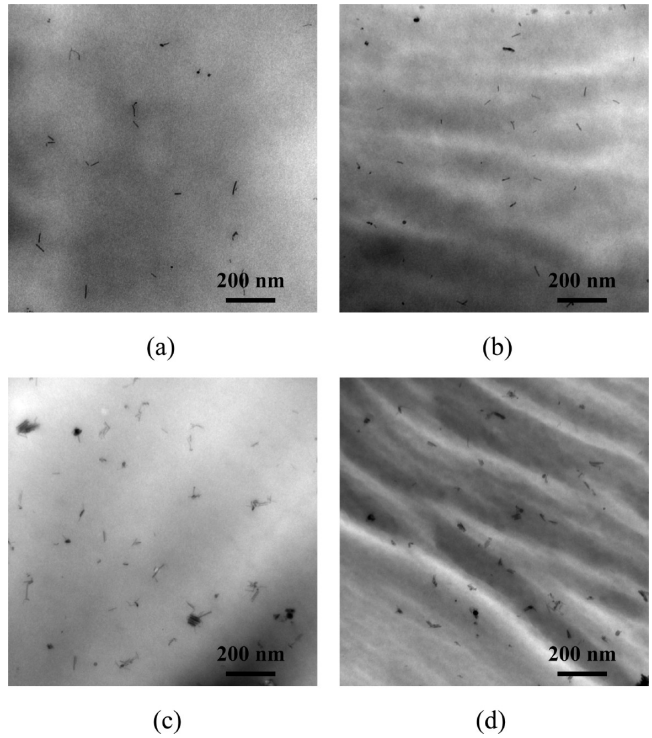

Figure 3. Dispersion of nanorods in PVP: (a) ϕ = 0.5%; (b) ϕ = 1%; (c) ϕ = 2%; and (d) ϕ = 4%. The rod length is 40.8 nm.

dispersion behavior of short nanorods in PVP, the long nanorods tend to form aggregates in the matrix (Figure 4, b, c, and d). The individual aggregates ranged in size from ~200 nm to several hundred nanometers, and the number of aggregates increased with an increase in the rod concentration.

dx.doi.org/10.1021/jp308723q | J. Phys. Chem. B 2013, 117, 5261−5270

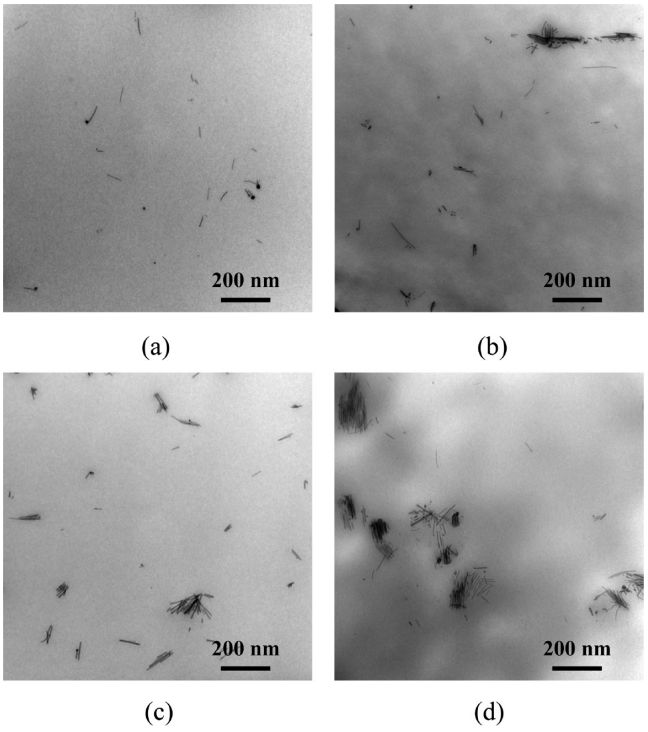

Figure 4. Dispersion of nanorods in PVP: (a) ϕ = 0.5%; (b) ϕ = 1%; (c) ϕ = 2%; and (d) ϕ = 4%. The rod length is 100.9 nm.

As indicated by our experiments, the pyridine-tethered nanorods uniformly dispersed in PVP for nanorods with a length of 20.9 and 40.8 nm. On the contrary, nanorods with a length of 100.9 nm formed extensive aggregation with increasing rod content.

Dispersion of Nanorods in Block Copolymer. In this section, the pyridine-tethered nanorods were mixed with PS-PVP and the effect of the rod length on the morphology of PS-PVP/nanorod composites was studied. The neat PS-PVP exhibited a lamellar structure. Without employing the surface ligand exchange procedure, nanorods were found to become clustering with the aggregated size much larger than the domain size of polymer microphase, causing macrophase separation of nanorods from block copolymer (data not shown). By ligand exchange process, nanorods afford to have surface ligand coverage of pyridine that enhances the interactions between nanorods and PVP blocks competing against the relatively strong interactions among magnetic nanorods. Figure 5 presents TEM cross section of lamellar composites with a rod length of 20.9 nm in the symmetric block copolymer. The white areas of the micrographs are segregated PS sequences, the gray areas are PVP phase, and the block spots are made of nanorods. The surface coverage of nanorods using pyridine was sufficiently high to prevent the contact of the rod surface and the nanorods were sequestered in the PVP phase. Above a threshold particle concentration ($\phi \sim 2\%$), nanorods failed to disperse individually in polymer phase and small aggregates of nanorods occurred. However, no extensive macrophase separation was observed. At ϕ = 4.0% (Figure 5d), the size of aggregates suppressed the domain size of PVP, causing the poor selection of nanorods in PS-PVP. However, the morphology of PS-PVP still exhibited a lamellar structure.

To complement theses results, we used SAXS to determine the structural features of these nanocomposites as shown in

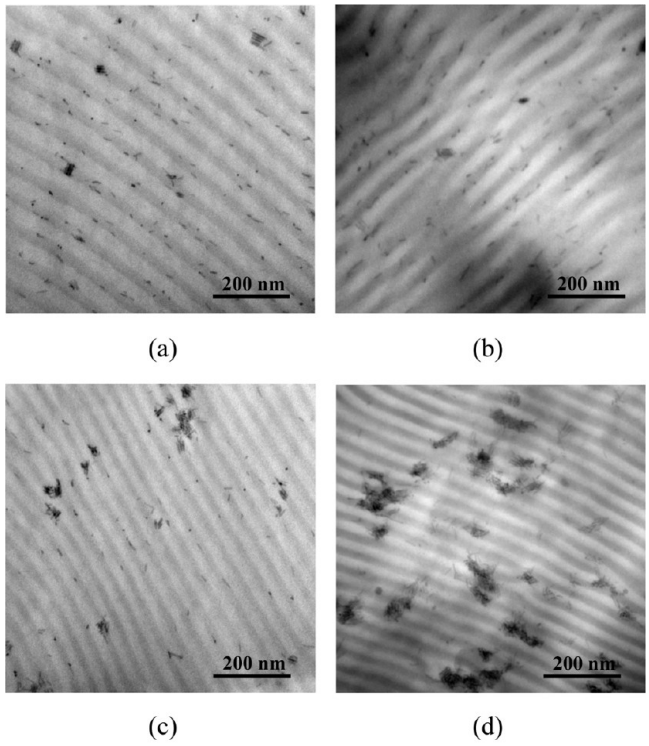

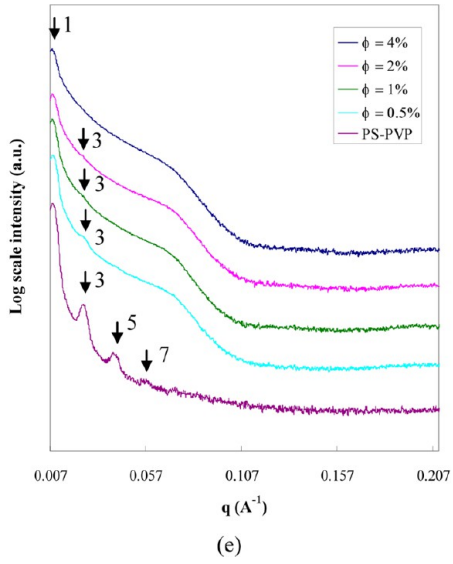

Figure 5. TEM images of PS-PVP/nanorod composites: (a) ϕ = 0.5%; (b) ϕ = 1%; (c) ϕ = 2%; and (d) ϕ = 4%. (e) SAXS profiles of PS-PVP/nanorod composites. The rod length is 20.9 nm.

Figure 5e. As expected, neat PS-PVP exhibited several orders of diffraction peaks corresponding to a highly ordered lamellar phase. The absence of even order reflections is due to the symmetry grounds for symmetric diblocks where the sublayers have equal thickness. For nanocomposites with ϕ = 0.5%, 1%, and 2%, it is clear from Figure 5e that these samples also exhibited a lamellar order, but we could see only two diffraction peaks that appear to be slightly broadened, implying the decrease in the ordering of the polymer phase. Another reason for the higher order peaks being invisible in the SAXS data might be due to the masking by the strong scattering signal from the nanorods in the high q region.[42] From Figure 5e, the domain size of lamellae calculated by Bragg law increased from

dx.doi.org/10.1021/jp308723q | J. Phys. Chem. B 2013, 117, 5261−5270

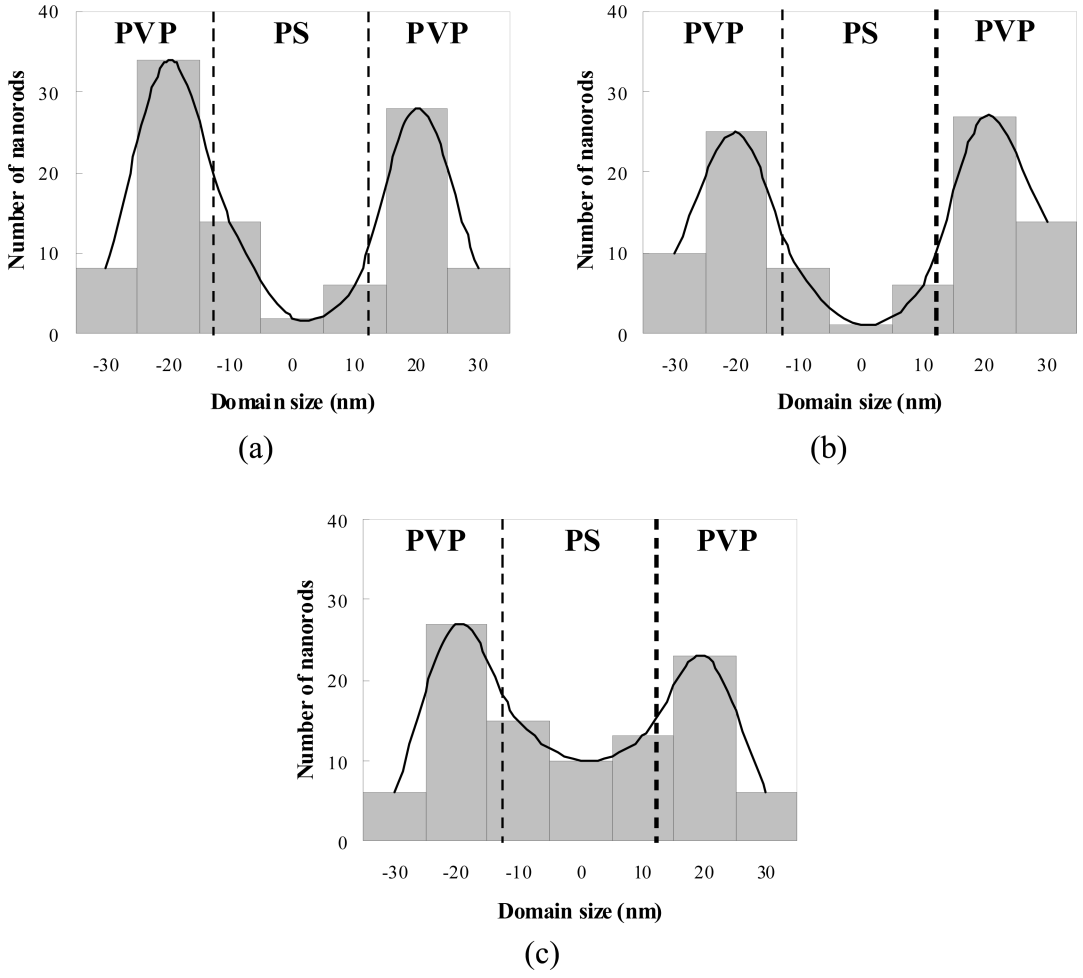

Figure 6. Dispersion of nanorods in PS-PVP: (a) ϕ = 0.5%; (b) ϕ = 1%; and (c) ϕ = 2%. The rod length is 20.9 nm. Data are averaged at a given position relative to zero.

75.2 nm for neat PS-PVP to 76.2, 76.8, and 77.4 nm for 0.5%, 1%, and 2% nanorods, respectively. This increase in domain size with an increased in rod concentration is associated with the confinement of nanorods in the preferred domains of block copolymer.[43]

Histograms of particle center location as a function of distance from the center of the PS domain are shown in Figure 6. As illustrated, the particle concentration is higher in the PVP domains. With increasing particle loading, the dispersion of nanorods in the PS domains increased, indicating that the particle selection in the preferred domains of PS-PVP reduced. We defined an alignment of the long axis of nanorods along the PS-PVP interface as zero angle and analyzed the orientation of nanorods with respect to the particle loading. As seen in Figure 7, most nanorods aligned parallel to the interface. At high particle loading, the number of parallel-organized nanorods reduced due to the poor selection of nanorods in the preferred domains of PS-PVP. These parallel aligned nanorods are attributed to the conformational entropy of polymer chains. When nanorods are randomly oriented in PS-PVP (Figure 8), nanorods cause chain stretching that decreases the conformational entropy of polymers. On the other hand, by aligning nanorods parallel to the interface between two microdomains, polymer chains can accommodate particles by moving apart rather than by stretching. Furthermore, localizing particles near the center of the compatible domain sacrifices translational entropy of the particles, but avoids an even larger chain stretching penalty incurred by distributing particle through the domain.[27] This conformational entropy justifies the organization of nanorods and hence the parallel organized nanorods along the interface of PS-PVP are obtained.

Figure 9 shows the organization of nanorods with the rod length of 40.8 nm in PS-PVP. In contrast to the PS-PVP/nanorod composites with the smaller rod length, the incorporation of longer nanorods in PS-PVP caused the dislocation and declination of composite microstructure and the longer nanorods preferred to locate at the dislocation and declination. The longer nanorods also reduced the selection of nanorods in the PVP domains by forming aggregates. These aggregates enhanced the fluctuation between PS and PVP interfaces and in turn caused the microstructure to lose its long-range order. Although the microstructure became poorly ordered, the incorporation of nanorods did not induce an order−disorder transition and a lamellar structure was still maintained at ϕ = 4%. Figure 9e compares the SAXS data of the neat PS-PVP and its composites with a rod length of 40.8 nm. Since the higher order peaks are not visible in the data due to the dominant SAXS signal from nanorods, it is difficult to determine the morphology of these composites. However, the ordering of these composites is obviously much poorer when compared to the composites with a rod length of 20.9 nm.

dx.doi.org/10.1021/jp308723q | J. Phys. Chem. B 2013, 117, 5261−5270

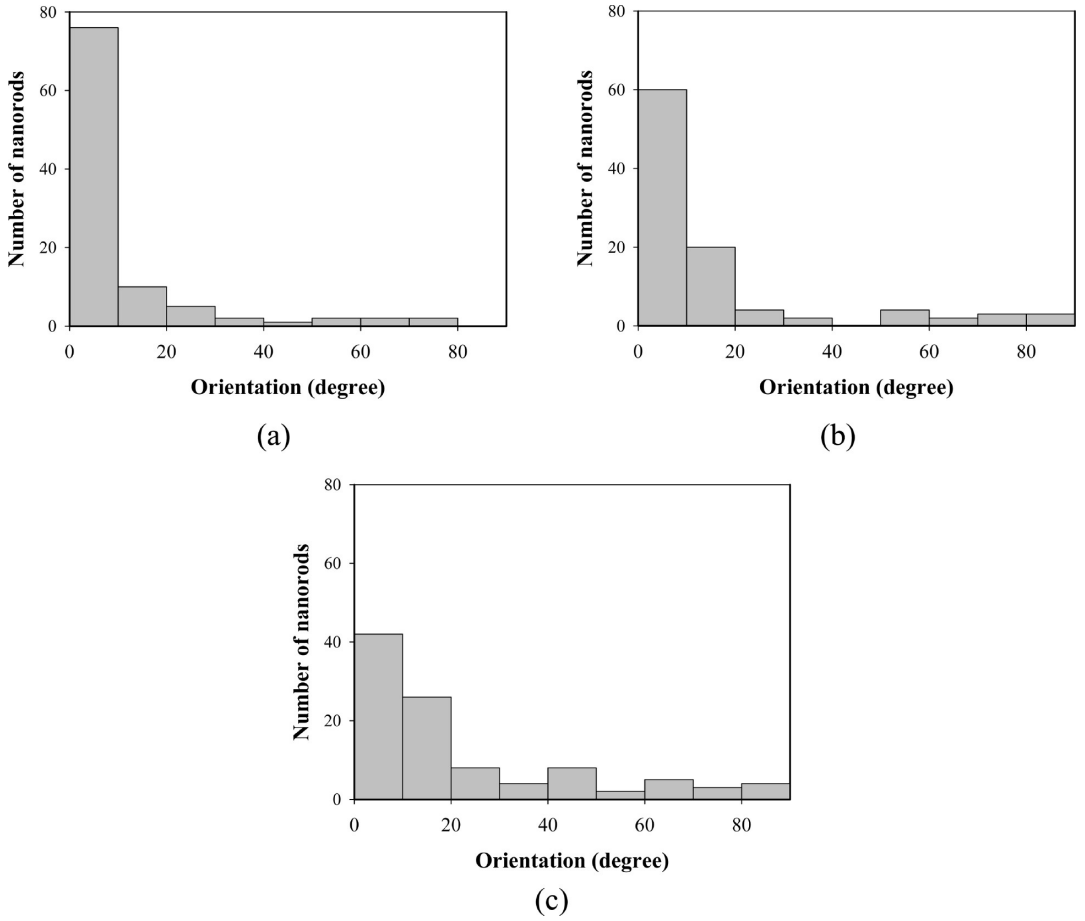

Figure 7. Orientation of nanorods in PS-PVP: (a) ϕ = 0.5%; (b) ϕ = 1%; and (c) ϕ = 2%. The rod length is 20.9 nm.

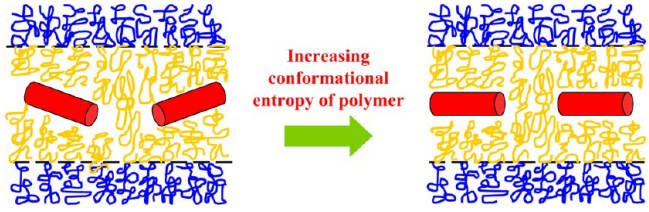

Figure 8. Schematics of the nanorods organized in block copolymer. Left, nanorods exhibit random orientation; and right, nanorods are parallel to the interface.

With further increasing rod length to 100.9 nm, nanorods formed extensive aggregation at ϕ = 0.5% as shown in Figure 10a. The formation of particle-rich regions enhanced the local concentration gradient of particles and it spontaneously tortured lamellae. With an increase in particle loading, Figure 10b reveals the morphology of block copolymer perturbed by the existence of rod aggregates. Meanwhile, the size of aggregates increased upon the addition of nanorods. Consequently, nanorods were expelled from the polymer phases and the structure of the composite lost its long-range order (Figure 10c). In the SAXS data in Figure 10d, the broad peak at $\sim q$ = 0.075 Å^{-1} provides evidence for the interparticle correlation between the nanorods in the segregated domains, suggesting the existence of rod aggregation. Such a correlation peak does not exist for composites with a rod length of 20.8 nm wherein the particles are dispersed in the PVP domains and only the form factor of particles is observed.

On the basis of the experimental results obtained, we could schematically represent the phase behavior of the block copolymer/nanorod mixtures as a function of rod length, as shown in Figure 11. Small nanorods could disperse selectively in the PVP domains and composites exhibited an ordered lamellar structure at low particle loading. At high particle loading, particles formed aggregation, causing the poor selection of nanorods in PS-PVP. It has to be pointed out that the critical particle concentration to form particle aggregation in this block copolymer/nanorod composite is much smaller than that in block copolymer/spherical nanorod composite as the latter is mostly larger than 10 wt %.[9] This is associated with the larger volume of nanorods. To manipulate a solid filler in the preferred domains of block copolymer, a small filler is able to distribute between the neighboring chains, creating a situation of wet brush. This wet brush swells the domains and does not diminish the conformational entropy of the system. On the contrary, when a large filler is incorporated into the preferred domain of block copolymer, it cannot be accommodated between the neighboring chains. Instead, chains need to stretch, causing dry brush. This dry brush reduces the conformational entropy and prevents particles from distribution in the domains. Eventually, particles form aggregation to release the chain stretching and to regain the conformational entropy.

For longer nanorods, the reduced entropy of polymer from incorporating nanorods disfavors mixing. In addition, due to both the higher van der Waals and magnetic interactions between longer nanorods, nanorods are easier to form aggregation. These aggregates increase the local concentration

dx.doi.org/10.1021/jp308723q | J. Phys. Chem. B 2013, 117, 5261−5270

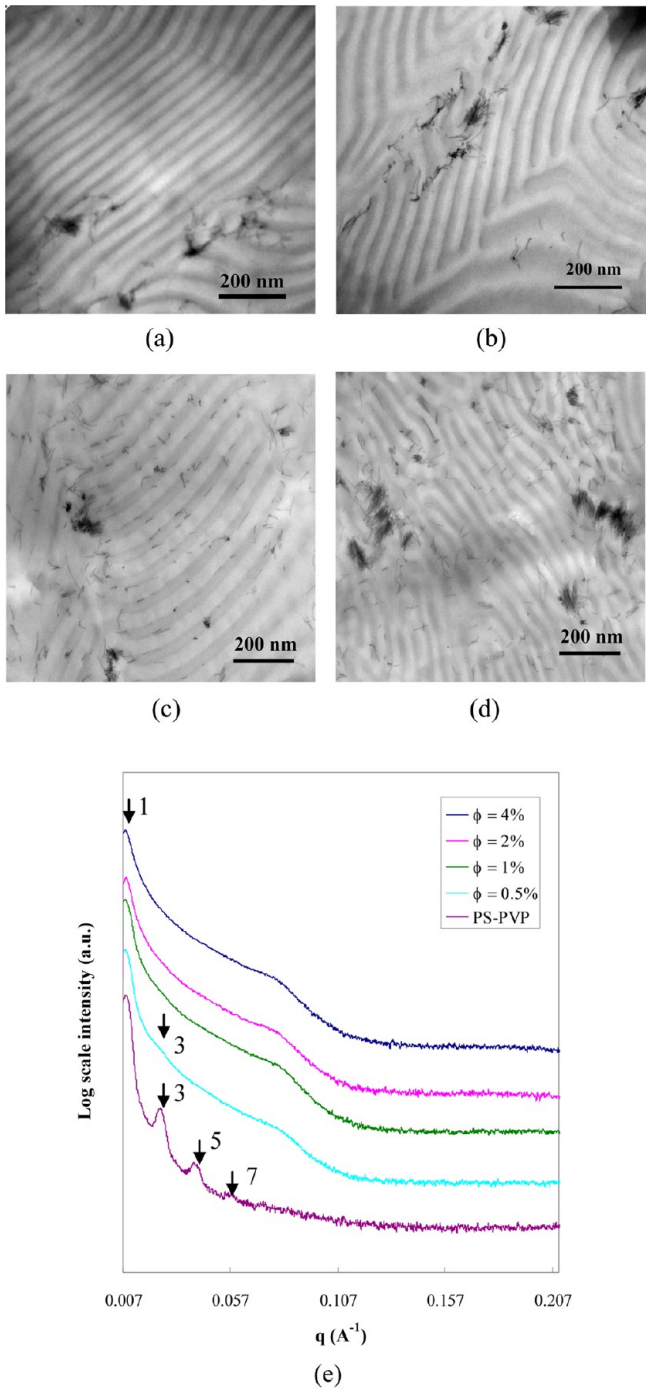

Figure 9. TEM images of PS-PVP/nanorod composites: (a) ϕ = 0.5%; (b) ϕ = 1%; (c) ϕ = 2%; and (d) ϕ = 4%. (e) SAXS profiles of PS-PVP/nanorod composites. The rod length is 40.8 nm.

gradient and adversely affect the long-range order in the system. Consequently, they perturb the morphology of block copolymer and induce a morphological transition from a well-ordered structure to a disordered structure (Figure 11).

Chen and Ma conducted a two-dimensional simulation of noninteracting nanorods dispersed in a symmetric block copolymer melt.[34] In the case of strong preferential wetting of rods by one component of the copolymer, the oriented ordering dynamics of the rods guided striped domain of copolymers with a parallel oriented arrangement. On the contrary, when the wetting strength was weak, the rods were not fully restricted in the preferred domains of block copolymer and the distribution of the rods was dispersive. He et al. performed dissipative particle dynamics simulations to predict the phase behavior of diblock copolymer/noninteracting nanorod composites and found that both the length and volume fraction of rods affect the morphology of the mixtures, the rod position distribution, and rod spatial orientation.[35] With a low volume fraction of nanorods, the nanorods tended to distribute dispersedly in the preferred domains and the spatial confinement from the lamellar structure of block copolymer strongly orientated the nanorods behaviors. With an increase in volume fraction of nanorods, the instinctive aggregates, as a result of rod anisotropy, drove the nanorods to distribute mainly in the domains with a relative free orientation. A further loading of nanorods led to a decrease in the uniform orientation of nanorods, dominated by the strong repulsion between a large number of nanorods. In our investigation on block copolymer/interacting nanorod composites, the dispersion state of magnetic nanorods and their assembly behavior in symmetric block copolymer are qualitatively consistent with the simulation results on block copolymer/noninteracting nanorod mixtures. Unlike block copolymer/noninteracting nanorod mixtures, the strong magnetic interactions between nanorods in block copolymer/interacting nanorod mixtures also caused rod aggregation with increasing rod length and concentration. This further induced macrophase separation of nanorods from the preferred domains of block copolymer. As a result, the ordered morphology was perturbed and the nanorods lost their uniform orientation.

In the block copolymer/nanorod composites, the spontaneous change in conformational entropy of polymer upon the addition of nanorods strongly influences on the composite morphology and the rod orientation. In addition to the conformational entropy of the polymer, we cannot exclude both the role of the van der Waals and magnetic interactions on the organization of magnetic nanorods in block copolymer. For small rod separations, the van der Waals interaction energy between parallel nanorods is given by[44]

$$W_{\mathrm{VDW}} = -\frac{AL\sqrt{d/2}}{24l^{2/3}} \quad (1)$$

Here, A is the Hamaker constant, which is $\sim 10^{-19}$ J for Fe-based materials in hydrocarbon,[45] d is the rod diameter, L is the rod length, and l is the minimum separation distance between particle surfaces. For the rod diameter (d) of ~4.5 nm and the closest center-to-center separation distance between nanorods (z) of ~7.0 nm (obtained from TEM and $l = z - d$ = 2.5 nm), the van der Waals interaction energy is about -3.3×10^{-20} J ($-5.3kT$, where k is the Boltzmann constant and T is 453 K), -6.5×10^{-20} J ($-10.3kT$), and -1.6×10^{-19} J ($-25.5kT$) for 20.9, 40.8, and 100.9 nm long nanorods, respectively. The negative values indicated that the nanorods exhibit attractive interaction, causing particle aggregation.

In order to estimate the magnetic interaction, the magnetic nanorods were assumed to follow a spherocylinder particle model with well-defined magnetic moments.[46] Assuming that the magnetic nanorods formed an antiparallel packing (a raftlike structure) when aggregated, the magnetic interaction energy between these nanorods developed by Aoshima and Satoh is simplified as

dx.doi.org/10.1021/jp308723q | J. Phys. Chem. B 2013, 117, 5261−5270

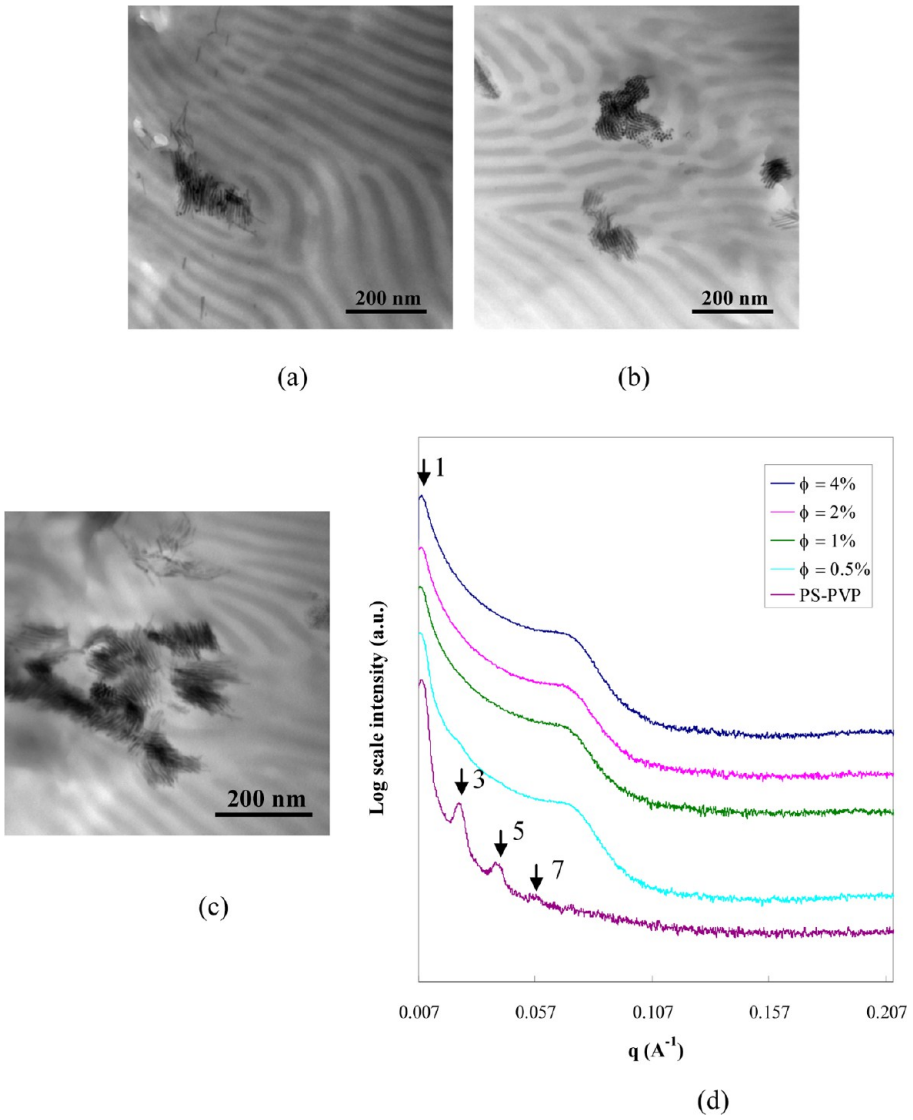

Figure 10. TEM images of PS-PVP/nanorod composites: (a) ϕ = 0.5%; (b) ϕ = 1%; and (c) ϕ = 2%. (d) SAXS profiles of PS-PVP/nanorod composites. The rod length is 100.9 nm.

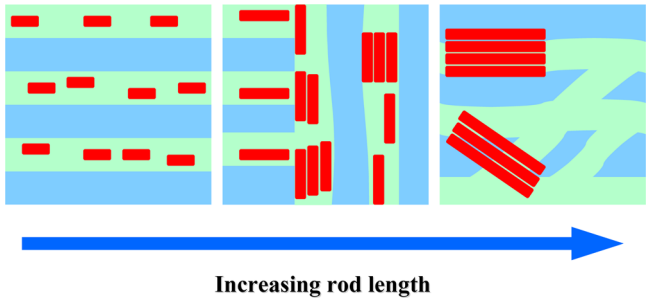

Figure 11. Schematics of the morphology of block copolymer/nanorod composite with different rod lengths.

$$u_{ij} = \frac{kT\lambda_0}{r_{ij}} \times \left[2\left(1 + \frac{r_p^2}{r_{ij}^2}\right)^{-1/2} - 2 \right] \quad (2)$$

Here, $\lambda_0 = \mu_0\mu^2/4\pi d^3kT$, μ_0 is the permeability of free space and has the value of $4\pi \times 10^{-7}$ J/A^{2}m, μ is the magnetic moment of one particle[47] (equal to its magnetic volume times the saturation magnetization and the saturation magnetization of Fe_2P is ~86 emu/g),[48] $r_{ij} = z/d$, and r_p is the aspect ratio of a nanorod. Thus, the potential energy between rods is calculated to be $-5.4kT$, $-25.1kT$, and $-172.2kT$ for 20.9, 40.8, and 100.9 nm long nanorods, respectively. Because both the van der Waals interaction energy and the magnetic interaction are comparable to the thermal fluctuation energy, we conclude that both attraction forces are responsible for rod aggregation.

CONCLUSION

We investigated the phase behavior of PS-PVP nanocomposites with the presence of pyridine-grafted Fe_2P nanorods. The morphology of composites strongly depends on the rod concentration and rod length. For short rod length, nanorods were sequestered in the PVP domains and aligned parallel to the interface between PS and PVP at low particle loading. The alignment of nanorods parallel to the PS−PVP interface can be understood by the entropic cost due to the incorporation of nanorods in the preferred domains. With nanorods parallel to the interface, polymer chains can accommodate particles by moving apart rather than by stretching. This avoids chain

dx.doi.org/10.1021/jp308723q | J. Phys. Chem. B 2013, 117, 5261−5270

stretching penalty and maximizes the entropy of the system. With increasing concentration of nanorods in the PVP domains, nanorods aggregated due to both the van der Waals interaction and the magnetic interaction, but the microphases did not experience any morphological transition. For long rod length, extensive rod aggregation occurred. The presence of these aggregates enlarged and modified the PVP domains, which in turn leads to the reduction of conformational entropic energy. As a result, the lamellar morphology gradually lost its long-range order with nanorods phase separated from the polymer phase upon an increase in rod concentration. This macrophase separation of nanorods and block copolymers leads to a disordered phase. The effect of magnetic nanorods on the morphology of block copolymer/nanorod composites, as clearly demonstrated in this study, can serve as guidance in controlling morphology and dispersing interacting particles in the fabrication of composites for different nanotechnological applications.

AUTHOR INFORMATION

Corresponding Author

*E-mail: tsunglo@mail.ncku.edu.tw. Tel.: +886-6-2757575, ext 62647. Fax: +886-6-2344496.

Notes

The authors declare no competing financial interest.

ACKNOWLEDGMENTS

This work is financially supported by the National Science Council in Taiwan with Grant No. NSC 98-2221-E-006-004-MY2.

REFERENCES

(1) Kryder, M. H. Status and Future of Magnetic Data Storage Technology. *Proc. Electrochem. Soc.* **2002**, *2002−2027*, 3−25.

(2) Sun, S.; Weller, D.; Murray, C. B. In *The Physics of Ultra-High-Density Magnetic Recording*; Plumer, J., van, E. K., Weller, D., Eds.; Springer-Verlag: New York, 2001; Vol. *41*, p 249.

(3) Black, C. T.; Murray, C. B.; Sandstrom, R. L.; Sun, S. Spin-dependent Tunneling in Self-Assembled Cobalt-Nanocrystal Superlattices. *Science* **2000**, *290*, 1131−1134.

(4) Gu, H.; Ho, P.-L.; Tsang, K. W. T.; Wang, L.; Xu, B. Using Biofunctional Magnetic Nanoparticles to Capture Vancomycin-Resistant Enterococci and Other Gram-positive Bacteria at Ultralow Concentration. *J. Am. Chem. Soc.* **2003**, *125*, 15702−15703.

(5) Huber, D. L. Synthesis, Properties, and Applications of Iron Nanoparticles. *Small* **2005**, *1*, 482−501.

(6) Elliott, D. W.; Zhang, W.-X. Field Assessment of Nanoscale Biometallic Particles for Groundwater Treatment. *Environ. Sci. Technol.* **2001**, *35*, 4922−4926.

(7) Takafuji, M.; Ide, S.; Ihara, H.; Xu, Z. Preparation of Poly(1-vinylimidazole)-Grafted Magnetic Nanoparticles and Their Application for Removal of Metal Ions. *Chem. Mater.* **2004**, *16*, 1977−1983.

(8) Lu, A.-H.; Salabas, E. L.; Schüth, F. Magnetic Nanoparticles: Synthesis, Protection, Functionalization, and Application. *Angew. Chem., Int. Ed.* **2007**, *46*, 1222−1244.

(9) Lo, C.-T.; Chao, C.-J. Synthesis and Characterization of Magnetic Nanoparticle/Block Copolymer Composites. *Langmuir* **2009**, *25*, 12865−12869.

(10) Darling, S. B.; Yufa, N. A.; Cisse, A. L.; Bader, S. D.; Sibener, S. J. Self-Organization of FePt Nanoparticles on Photochemically Modified Diblock Copolymer Templates. *Adv. Mater.* **2005**, *17*, 2446−2450.

(11) Park, M. J.; Char, K.; Park, J.; Hyeon, T. Effect of the Casting Solvent on the Morphology of Polystyrene-b-isoprene) Diblock Copolymer/Magnetic Nanoparticle Mixtures. *Langmuir* **2006**, *22*, 1375−1378.

(12) Park, M. J.; Park, J.; Hyeon, T.; Char, K. Effect of Interacting Nanoparticles on the Ordered Morphology of Block Copolymer/Nanoparticle Mixtures. *J. Polym. Sci., Part B: Polym. Phys.* **2006**, *44*, 3571−3579.

(13) Xu, C.; Ohno, K.; Ladmiral, V.; Composto, R. J. Dispersion of Polymer-grafted Magnetic Nanoparticles in Homopolymers and Block Copolymers. *Polymer* **2008**, *49*, 3568−3577.

(14) Xu, C.; Ohno, K.; Ladmiral, V.; Milkie, D. E.; Kikkawa, J. M.; Composto, R. J. Simultaneous Block Copolymer and Magnetic Nanoparticle Assembly in Nanocomposite Films. *Macromolecules* **2009**, *42*, 1219−1228.

(15) Chiu, J. J.; Kim, B. J.; Kramer, E. J.; Pine, D. J. Control of Nanoparticle Location in Block Copolymers. *J. Am. Chem. Soc.* **2005**, *127*, 5036−5037.

(16) Kim, B. J.; Chiu, J. J.; Yi, G.-R.; Pine, D. J.; Kramer, E. J. Nanoparticle-Induced Phase Transitions in Diblock-Copolymer Films. *Adv. Mater.* **2005**, *17*, 2618−2622.

(17) Bockstaller, M. R.; Thomas, E. L. Proximity Effects in Self-Organized Binary Particle-block Copolymer Blends. *Phys. Rev. Lett.* **2004**, *93*, 166106.

(18) Lo, C.-T. ; Lee, B.; Pol, V. G.; Dietz-Rago, N. L.; Seifert, S.; Winans, R. E.; Thiyagarajan, P. Effect of Molecular Properties of Block Copolymers and Nanoparticles on the Morphology of Self-Assembled Bulk Nanocomposites. *Macromolecules* **2007**, *40*, 8302−8310.

(19) Lo, C.-T.; Lee, B.; Dietz-Rago, N. L.; Winans, R. E.; Thiyagarajan, P. Strategy for Better Ordering in Diblock Copolymer Based Nanocomposites. *Macromol. Rapid Commun.* **2007**, *28*, 1607−1612.

(20) Lin, Y.; Böker, A.; He, J.; Sill, K.; Xiang, H.; Abetz, C.; Li, X.; Wang, J.; Emrick, T.; Long, S.; Wang, Q.; Balazs, A.; Russell, T. P. Self-Directed Self-Assembly of Nanoparticle/Copolymer Mixtures. *Nature* **2005**, *434*, 55−59.

(21) Zhang, Q.; Gupta, S.; Emrick, T.; Russell, T. P. Surface-Functionalized CdSe Nanorods for Assembly in Diblock Copolymer Templates. *J. Am. Chem. Soc.* **2006**, *128*, 3898−3899.

(22) Yeh, S.-W.; Wei, K.-H.; Sun, Y.-S.; Jeng, U-S.; Liang, K. S. CdS Nanoparticles Induce a Morphological Transformation of Poly(styrene-b-4-vinylpyridine) from Hexagonally Packed Cylinders to a Lamellar Structure. *Macromolecules* **2005**, *38*, 6559−6565.

(23) Schulz, M. F.; Khandpur, A. K.; Bates, F. S.; Almdal, K.; Mortensen, K.; Hajduk, D. A.; Gruner, S. M. Phase Behavior of Polystyrene-poly(2-vinylpyridine) Diblock Copolymers. *Macromolecules* **1996**, *29*, 2857−2867.

(24) Lee, J. Y.; Thompson, R. B.; Jasnow, D.; Balazs, A. C. Effect of Nanoscopic Particles on the Mesophase Structure of Diblock Copolymers. *Macromolecules* **2002**, *35*, 4855−4858.

(25) Huh, J.; Ginzburg, V. V.; Balazs, A. C. Thermodynamic Behavior of Particle/Diblock Copolymer Mixtures: Simulation and Theory. *Macromolecules* **2000**, *33*, 8085−8096.

(26) Bockstaller, M. R.; Lapetnikov, Y.; Margel, S.; Thomas, E. L. Size-selective Organization of Enthalpic Compatibilized Nanocrystals in Ternary Block Copolymer/Particle Mixtures. *J. Am. Chem. Soc.* **2003**, *125*, 5276−5277.

(27) Thompson, R. B.; Ginzburg, V. V.; Matsen, M. W.; Balazs, A. C. Predicting the Mesophases of Copolymer-Nanoparticle Composites. *Science* **2001**, *292*, 2469−2472.

(28) Thompson, R. B.; Ginzburg, V. V.; Matsen, M. W.; Balazs, A. C. Block Copolymer-Directed Assembly of Nanoparticles: Forming Mesoscopically Ordered Hybrid Materials. *Macromolecules* **2002**, *35*, 1060−1071.

(29) Tsutsumi, K.; Funaki, Y.; Hirokawa, Y.; Hashimoto, T. Selective Incorporation of Palladium Nanoparticles into Microphase-Separated Domains of Poly(2-vinylpyridine)-block-polyisoprene. *Langmuir* **1999**, *15*, 5200−5203.

(30) Hashimoto, T.; Harada, M.; Sakamoto, N. Incorporation of Metal Nanoparticles into Block Copolymer Nanodomains via In-situ

Reduction of Metal Ions in Microdomain Space. *Macromolecules* **1999**, *32*, 6867−6870.
(31) Warren, S. C.; Disalvo, F. J.; Wiesner, U. Nanoparticle-Tuned Assembly and Disassembly of Mesostructured Silica Hybrids. *Nat. Mater.* **2007**, *6*, 156−161.
(32) Sorensen, C. M. In *Magnetism in Nanoscale Materials in Chemistry*; Klabunde, K. J., Ed.; Wiley-Interscience Publication: New York, 2001.
(33) Bockstaller, M. R.; Mickiewicz, R. A.; Thomas, E. L. Block Copolymer Nanocomposites: Perspectives for Tailored Functional Materials. *Adv. Mater.* **2005**, *17*, 1331−1349.
(34) Chen, K.; Ma, Y.-Q. Ordering Stripe Structures of Nanoscale Rods in Diblock Copolymer Scaffolds. *J. Chem. Phys.* **2002**, *116*, 7783−7786.
(35) He, L.; Zhang, L.; Liang, H. Mono- or Bidisperse Nanorods Mixtures in Diblock Copolymers. *Polymer* **2010**, *51*, 3303−3314.
(36) Deshmukh, R. D.; Liu, Y.; Composto, R. J. Two-Dimensional Confinement of Nanorods in Block Copolymer Domains. *Nano Lett.* **2007**, *7*, 3662−3668.
(37) Murphy, C. J.; Orendorff, C. J. Alignment of Gold Nanorods in Polymer Composites and on Polymer Surfaces. *Adv. Mater.* **2005**, *17*, 2173−2177.
(38) Park, J.; Koo, B.; Yoon, K. Y.; Hwang, Y.; Kang, M.; Park, J.-G.; Hyeon, T. Generalized Synthesis of Metal Phosphide Nanorods via Thermal Decomposition of Continuously Delivered Metal-phosphine Complexes Using a Syringe Pump. *J. Am. Chem. Soc.* **2005**, *127*, 8433−8440.
(39) Gupta, S.; Zhang, Q.; Emrick, T.; Russell, T. P. "Self-Corralling" Nanorods Under an Applied Electric Field. *Nano Lett.* **2006**, *6*, 2066−2069.
(40) Kim, B. J.; Bang, J.; Hawker, C. J.; Kramer, E. J. Effect of Areal Chain Density on the Location of Polymer-Modified Gold Nanoparticles in a Block Copolymer Template. *Macromolecules* **2006**, *39*, 4108−4114.
(41) Chiu, J. J.; Kim, B. J.; Yi, G.-R.; Bang, J.; Kramer, E. J.; Pine, D. J. Distribution of Nanoparticles in Lamellar Domains of Block Copolymers. *Macromolecules* **2007**, *40*, 3361−3365.
(42) Lee, B.; Lo, C.-T.; Seifert, S.; Dietz-Rago, N. L.; Winans, R. E.; Thiyagarajan, P. Anomalous Small-Angle X-ray Scattering Characterization of Bulk Block Copolymer/Nanoparticle Composites. *Macromolecules* **2007**, *40*, 4235−4243.
(43) Matsushita, Y.; Torikai, N.; Mogi, Y.; Noda, I.; Han, C. C. Localization of a Homopolymer Dissolved in a Lamellar Structure of a Block-Copolymer Studied by Small-Angle Neutron-Scattering. *Macromolecules* **1993**, *26*, 6346−6349.
(44) Israelachvili, J. N. In *Intermolecular and surface forces*, 2nd ed.; Academic Press: London, 1992.
(45) Rosensweig, R. E. In *Ferrohydrodynamics*; Cambridge University Press: Cambridge, 1985.
(46) Aoshima, M.; Satoh, A. Two-Dimensional Monte Carlo Simulations of a Colloidal Dispersion Composed of Rod-like Ferromagnetic Particles in the Absence of an Applied Magnetic Field. *J. Colloid Interface Sci.* **2006**, *293*, 77−87.
(47) Berkovski, B.; Bashtovoy, V. In *Magnetic Fluids and Applications Handbook*; Begel House Inc.: New York, 1996.
(48) Bellavance, D.; Mikkelsen, J.; Wold, A. Preparation and Properties of Fe_2P. *J. Solid State Chem.* **1970**, *2*, 285−290.